Acta Crystallographica Section D
Biological Crystallography
ISSN 0907-4449

Difference density quality (*DDQ*): a method to assess the global and local correctness of macromolecular crystal structures

Focco van den Akker[a,b]† and Wim G. J. Hol[a,b,c]*

[a]Department of Biochemistry, University of Washington, Seattle, WA 98195-7420, USA, [b]Department of Biological Structure, University of Washington, Seattle, WA 98195-7420, USA, and [c]Howard Hughes Medical Institute and Biomolecular Structure Center, University of Washington, Seattle, WA 98195-7420, USA

† Present address: Department of Molecular Biology/NC-20, Cleveland Clinic Foundation, Cleveland, OH 44195, USA.

Correspondence e-mail: hol@gouda.bmsc.washington.edu

Received 11 December 1997
Accepted 19 May 1998

Methods for the evaluation of the accuracy of crystal structures of proteins and nucleic acids are of general importance for structure–function studies as well as for biotechnological and biomedical research based upon three-dimensional structures of biomacromolecules. The structure-validation program *DDQ* (difference-density quality) has been developed to complement existing validation procedures. The *DDQ* method is based on the information present in a difference electron-density map calculated with the water molecules deliberately omitted from the structure-factor calculation. The quality of a crystal structure is reflected in this difference map by (i) the height of solvent peaks occurring at physical chemically reasonable positions with respect to protein and ligand atoms and (ii) the number and height of positive and negative 'shift' peaks next to protein atoms. The higher the solvent peaks and the lower the shift peaks, the better the structure is likely to be. Moreover, extraneous positive density due to an incomplete molecular model is also monitored, since this is another indicator of imperfections in the structure. Automated analysis of these types of features in difference electron densities is used to quantify the local as well as global accuracy of a structure. In the case of proteins, the *DDQ* structure-validation method is found to be very sensitive to small local errors, to omitted atoms and also to global errors in crystal structure determinations.

1. Introduction

Macromolecular structure validation is of general importance and has recently been a topic of vigorous discussion (Brändén & Jones, 1990; Hooft *et al.*, 1996; Jones *et al.*, 1996; Kleywegt & Brünger, 1996; Kleywegt & Jones, 1996). Current structure-validation methods can be divided into two categories. The first category uses only the coordinates to assess the accuracy of the structure and does not use experimentally observed diffraction data. Examples of programs that implement such methods are those which only check for proper stereochemistry including *PROCHECK* (Lawskowski *et al.*, 1993), *WHATIF* (Hooft *et al.*, 1996) and the Ramachandran plot (Ramakrishnan & Ramachandran, 1965; Kleywegt & Jones, 1996). Other validation methods in this first category look at the degree of chemically sensible local environments as implemented in the *3D1D* profile (Lüthy *et al.*, 1992). Others check the statistical distribution of atomic distances, as implemented in *ProsaII* (Sippl, 1993) and *Errat* (Colovos & Yeates, 1993), investigate deviations from standard atomic volumes (Pontius *et al.*, 1996) or look into atomic solvation preferences (Holm & Sander, 1992). The second category of methods uses the measured diffraction data in some form to

check the coordinates. The advantage is input from experimental data in evaluating models, but such methods are limited to structures determined by one particular technique, in our case X-ray crystallography. These latter methods include the conventional R factor, the $R_{\rm free}$ (Brünger, 1992), the real-space R factor (Jones *et al.*, 1991) and quantitative estimations of the coordinate error obtained from, for example, the Luzzati plot (Luzzati, 1952), the σ_A plot (Read, 1986, 1990) or the diffraction-data precision indicator (Cruickshank, 1996). These two categories of crystal structure-validation methods each have different advantages and disadvantages. We present here a method, difference-density quality evaluation (*DDQ*), which is in some sense a hybrid procedure.

DDQ is a new method for the automatic assessment of the local and global correctness of a macromolecular crystal structure combining diffraction data, in the form of a particular type of difference electron-density map, with the known preferred positions of water molecules with respect to protein, nucleic acid and ligand atoms. The method is based on the information found in ($|F_{\rm obs}| - |F_{\rm calc}|$) difference electron-density maps in which water molecules are deliberately omitted from the structure-factor calculation. These maps are hereafter also referred to as 'hydrated difference maps' or HDMs. Such difference electron-density distributions provide a wealth of information concerning the local and global accuracy of the crystal structure such as the following.

(i) Hydrophilic, and to some extent also hydrophobic, atoms that are correctly positioned within the structure can make favourable interactions with water molecules appearing as positive peaks in these difference maps. Analysis of such water peaks can be carried out using the available detailed biophysical information about the hydration of atoms in protein structures. The positions of these water peaks are an indicator of the correctness of the atomic positions of the amino-acid residues surrounding the waters, and the height of the water peaks is an indicator of the quality of the phases, and thus the overall correctness, of the crystal structure.

(ii) Atoms that are either completely mispositioned, slightly misplaced, or which have an incorrect temperature factor or occupancy assigned to them, will have negative and/or positive density peaks in their vicinity (Stout & Jensen, 1989) called 'shift peaks'. The height of these shift peaks is also dependent on the phase error and thus on the overall correctness of the model.

(iii) Segments of the structure not included in the model but present in the crystal are likely to show up as extra positive electron-density features. Significant amounts of 'unaccounted' positive density is an indicator of shortcomings of the model.

The concept of using a difference density map as a tool for locating positional errors in macromolecular structures is not new and is used by virtually every crystallographer, but hardly ever in an automated quantitative manner except perhaps by the program *SHELXL*, which provides a list of positive and negative peaks located near atoms of the model (Sheldrick, 1995). Our program *DDQ*, described herein, attempts to go a step further in combining the information in the hydrated difference map with biophysical information about protein hydration as a tool for the local and global evaluation of a crystal structure in an automated fashion. Therefore, *DDQ* allows not only very fast localization of problematic regions but also validation of correct regions. In addition, the occurrence of peaks in each of the three categories listed above [*i.e.* many strong water peaks in category (i), few shift peaks in category (ii) and no extra peaks in category (iii)] can be used as a quantitative measure for judging the global quality of the structure.

Our structure-verification method relies on the accuracy of the information in the hydrated difference Fourier. A difference map has an inherent advantage over a normal map, in that the errors in a difference Fourier are significantly smaller than in a normal Fourier map (Henderson & Moffat, 1971). An additional advantage of using a difference Fourier for structure validation is that its strongest peaks reveal where the largest deviations can be found between the model and the correct structure. It appears that the automatic detailed analysis of the difference Fourier map is a powerful tool for the validation of crystal structures at both a local and global level.

We would like to mention that the original source of inspiration for the creation of the *DDQ* method was hidden in Figs. 6(*a*) and 6(*b*) in Goodsell *et al.* (1995). These figures display the same difference electron density but with different postulated binding modes for the drug netropsin when complexed to DNA. The fit of netropsin in the density was obviously better for binding mode I than for the proposed binding mode II. Goodsell *et al.* concluded, partly from these figures,that the binding mode I of netropsin was indeed the correct one. However, the same difference electron-density figure also showed features not highlighted by these authors: the presence of unbiased water peaks which were at approximately the correct hydrogen-bonding distance and van der Waals distance with respect to netropsin in binding mode I but not with respect to binding mode II. This led to the realisation that water peaks in difference maps can aid structure validation. Eventually, this resulted in *DDQ*, which combines difference density and biophysical information to assess the accuracy of biomacromolecular crystal structures.

2. Principles of the difference-density quality (*DDQ*) structure-validation method

Our procedure starts, as mentioned above, with a hydrated difference map. Based on features in the HDM three local indicators are calculated: (i) DDQ-W, evaluating positive water peaks surrounding the protein molecule, (ii) DDQ-P, reflecting the positive peaks near protein atoms and (iii) DDQ-N, reflecting the occurrence of negative peaks near protein atoms. Based on these three indicators – which are first calculated per atom, then summed per side-chain, main-chain and hetero (*i.e.* a ligand or substrate) moiety and finally averaged over the entire structure – local as well as global structure-quality indicators are derived. Another global

Table 1
Distance parameters used to calculate the DDQ-P, DDQ-N and DDQ-W scores.

For the most common atoms, water-distance information is available and their source is listed. If no references could be found, the relevant distances were calculated by addition of the radius of oxygen to their cation or van der Waals radius. The $RMAX_p$ value can be calculated from this table: $RMAX_p = R_{midp} - R_{width}$. In most cases the $RMAX_n$ and $RMAX_p$ are identical, although not for every atom. The latter can be explained as follows: it seems unlikely that a negative peak at 2.6 Å from a C atom is due incorrect placement of that atom, as it is most likely to arise from the misplacement of a neighboring atom. However, a positive peak at, for example, 2.7 Å distance from a carbon atom could indicate either that the atom is located too close to a real water peak or that an atom bonded to this atom has been omitted. Either case constitutes an error and, in order to detect these, the $RMAX_p$ value is larger than the $RMAX_n$ value for certain specific atoms.

Atom type	Hydrogen-bond potential flag	$RMAX_n$†	R_{midp}‡	R_{width}§	Reference
O	1	2.4	2.9	0.5	Thanki *et al.* (1988); Roe & Teeter (1993)
N	1	2.4	3.0	0.5	Thanki *et al.* (1988); Roe & Teeter (1993)
C	0	2.4	4.0	1.0	Walshaw & Goodfellow (1993)
S	1	2.4	3.5	0.5	Gregoret *et al.* (1991)
Ca	1	2.1	2.4	0.3	McPhalen *et al.* (1991)
P¶	0	3.3	3.3	0.0	Calculated: van der Waals radius + 1.4 Å
Mg	1	1.8	2.1	0.3	Calculated: cation radius + 1.4 Å
Zn	1	1.8	2.1	0.3	Calculated: cation radius + 1.4 Å

measure for the quality of the structural model is based on the amount of positive 'extraneous' difference density. This is defined as positive difference density that is neither near protein atoms nor at potential water positions, and is possibly representing either missing parts of the structure, or cofactors, substrates, inhibitors *etc.* The following sections provide a detailed description of our hydrated difference map-based structure validation method, followed by the application of the method to several test cases.

2.1. Local quality indicators

2.1.1. The DDQ-W score. The presence of a correctly positioned positive water peak near a protein atom is taken as an indication for a high confidence in the placement of that atom (please note that a *high* DDQ-W score suggests *higher* confidence in model quality while *high* DDQ-P and DDQ-N scores, to be defined later, correspond to *lower* confidence in the correctness of the model). A favourable $DDQ\text{-}W_{polar}$ score is calculated for polar atoms which are at hydrogen-bonding distance from a probable water peak in the hydrated difference map. In addition, a favourable $DDQ\text{-}W_{apolar}$ score is assigned to apolar atoms which are at the appropriate van der Waals distance of a confidently assigned water peak.

An important first step before calculating DDQ-W is to determine which (non-protein) HDM peaks are most likely to be real water peaks and which positive peaks are due to model errors or unassigned protein moieties and should, therefore, be ignored. This evaluation is carried out in *DDQ* by examining the local environment of each difference density peak. Firstly, if there are any other positive or negative electron-density peaks within 2.4 Å of the positive HDM peak under consideration, it is no longer considered to be a potential water peak. Secondly, if the density peak is within a certain distance ($RMAX_p$) of any particular atom it is also no longer considered to be a water, as it is most likely to be a shift peak. Thirdly, the peak must have the proper geometry and distance from a nearby hydrogen-bond donor and/or acceptor atom(s) in the model, as has been characterized for polar groups in proteins and DNA (Baker & Hubbard, 1984; Thanki *et al.*, 1988; Roe & Teeter, 1993; Umrania *et al.*, 1995) or be at the proper distance from a hydrophobic atom (Walshaw & Goodfellow, 1993). These three different requirements appear to make the number of incorrectly assigned water peaks very small.

The carefully checked water peaks in the hydrated difference map are subsequently used to calculate a $DDQ\text{-}W_{polar}$ score for nearby polar protein atoms. The $DDQ\text{-}W_{polar}$ score of an atom is based on the relative peak height, the hydrogen-bond distance, the hydrogen-bond geometry, the temperature factor of the atom and a measure for the confidence in the correctness of the water peak. Each of these factors is a separate term when calculating the $DDQ\text{-}W_{polar}$ score for a polar atom i,

$$\mathrm{DDQ\text{-}W_{polar}} = (\rho_p - 2)^2 \times \mathrm{NHB} \times \mathrm{sANG} \times \left[\frac{R_{width}^2 - (R_{midp} - R_i)^2}{R_{width}^2}\right] \times \left(1 - \frac{B_i}{2B_{max}}\right), \quad (1)$$

where ρ_p is the relative HDM peak height in σ (only peaks above 3.0σ are used, resulting in values of one and higher for the peak-height term), NHB is the total number of hydrogen bonds in which that particular potential water is involved, sANG is the score ($0 < \mathrm{sANG} < 1$) for the angular position of the water position around polar atoms (see Fig. 1), R_{midp} is the midpoint of the hydrogen-bond distance distribution in Å (Table 1), R_{width} is the width of hydrogen-bond distance distribution in Å (Table 1), R_i is the distance in Å from difference peak to atom i, B_{max} is the maximum temperature factor (set to 100 Å^2) and B_i is the temperature factor in Å^2 of atom i; in the case that $B_i > B_{max}$ then $B_i = B_{max}$.

The distance-dependence term of the $DDQ\text{-}W_{polar}$ score is different for different polar-atom types, in order to account for the fact that each polar-atom type has its own optimal hydrogen-bond distance. For example, the average hydrogen-bond distance involving waters has been found to be 2.88 Å

for O and 2.95 Å for N atoms (Roe & Teeter, 1993). Besides the optimal distance, the width of the distribution of observed hydrogen-bond distances around the average distance for O atoms and N atoms was observed to be approximately 0.5 Å (Baker & Hubbard, 1984; Thanki *et al.*, 1988). Our method uses these experimental observations to calculate the DDQ-W score as a function of the distance between a potential solvent HDM peak and a polar atom. Each atom type is given its unique optimal midpoint distance to a potential solvent HDM peak ($R_{\rm midp}$) and width ($R_{\rm width}$), as listed in Table 1. The distance-dependent term in DDQ-$W_{\rm polar}$ is a parabolic curve with a score of 1.0 if R_i is equal to the midpoint distance and a value of 0.0 at $R_{\rm midp} \pm R_{\rm width}$. No DDQ-W score is calculated if R_i does not fall in this range.

The angular-dependence term of the DDQ-$W_{\rm polar}$ score is also based on experimental observations (Thanki *et al.*, 1988; Umrania *et al.*, 1995) and is similar to, but more general than, the angular dependence used in the solvent-prediction program *AQUARIUS* (Pitt & Goodfellow, 1991).

The measure of confidence in the correctness of the water peaks is included as a separate term in the DDQ-$W_{\rm polar}$ score. This term is made dependent on the total number of hydrogen-bond interactions (NHB) in which the positive water peak under consideration is involved. The rationale for this is that a potential water molecule which makes three hydrogen bonds in the crystal structure has a higher probability of actually being a water than if it makes only a single hydrogen bond. Consequently, residues involved in hydrogen-bond interactions with such a water should have a higher probability of being correctly positioned. The temperature-factor term is included in the DDQ-$W_{\rm polar}$ score to damp the score for atoms with very high temperature factors. The reasoning is that an atom with a B factor of, for example, 100 Å^2 should not receive the same high confidence as an atom with a B factor of 15 Å^2 when both are positioned optimally with respect to a positive water difference peak in the HDM. The B-factor-dependent term was considered to be the least important when calculating DDQ-W, and ranges therefore only between 0.5 and 1.0.

As mentioned above, our method also uses the presence of well established water peaks (*i.e.* those being engaged in one or more hydrogen bonds) in the HDM to assess the correctness in the positions of non-polar C atoms, even though these atoms cannot provide a hydrogen-bond donor or acceptor. The rationale is that the observed presence of positive water peaks near C atoms (Walshaw & Goodfellow, 1993) provides additional structural information and can be used to aid in validating the positions of hydrophobic atoms. This validation is implemented as the DDQ-$W_{\rm apolar}$ score. This score is similar to the DDQ-$W_{\rm polar}$ score but has fewer terms,

$$\text{DDQ-W}_{\rm apolar} = 0.25(\rho_p - 2)^2 \times \left[\frac{R_{\rm width}^2 - (R_{\rm midp} - R_i)^2}{R_{\rm width}^2}\right] \times \left(1 - \frac{B_i}{2B_{\rm max}}\right), \quad (2)$$

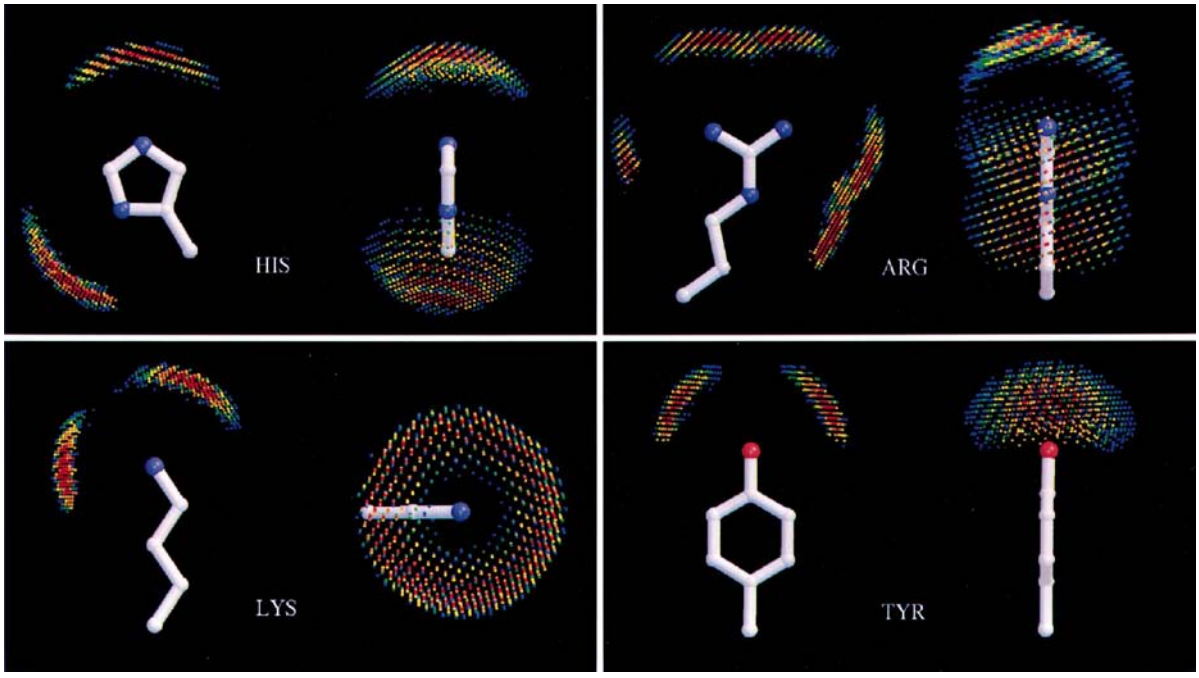

Figure 1
The angular and distance dependency of the DDQ-W score concerning the location of waters for several polar side chains is shown. The following overall geometry term P, which approximates the probability of finding waters at a particular position, is calculated on a grid with a spacing of 0.3 Å: $P = s\theta \times s\psi[R_{\rm width}^2 - (R_{\rm midp} - R_i)^2]/R_{\rm width}^2$. Only grid points with a value greater than 0.5 are shown for clarity. The side chains of His, Arg, Lys and Tyr are shown in front view (slabbed for clarity) and side view (not slabbed). The colors blue, green, yellow, orange and red are indicative of overall geometry-term values between 0.5–0.6, 0.6–0.7, 0.7–0.8, 0.8–0.9 and 0.9–1.0, respectively.

where ρ_p, B_i, B_{max}, R_i, R_{midp} and R_{width} are as defined for DDQ-W_{polar}. The R_{midp} and R_{width} values for C atoms can be found in Table 1.

The distance distribution of water around C atoms has previously been analyzed and found to range from 3.0 to 5.0 Å with a maximum around 4.0 Å (Walshaw & Goodfellow, 1993). No angular-dependence term is used in this case, even though some angular preferences were found for the solvent distribution around alanine and phenylalanine residues (Walshaw & Goodfellow, 1993). Since no directional hydrogen-bond interactions are made, the DDQ-W_{apolar} score is down-weighted by 0.25 compared to the DDQ-W_{polar} score. This weighting factor serves to give greater importance to polar atoms (which are engaged in directional hydrogen bonds) when assigning the confidence in the position of all atoms in a crystal structure.

2.1.2. DDQ-P and DDQ-N scores. The occurrence of positive and negative shift peaks close to a protein atom indicates an incorrect position, temperature factor or occupancy of that atom (and/or nearby atoms). Besides shift peaks, two other potential reasons can account for the presence of undesirable positive peaks near protein atoms: an atom either is positioned too close to a real water peak or is bonded to an atom which was not included in the model. When using these shift peaks to validate a model, it is obvious that their individual relative peak heights as well as the distances between the atoms and the peaks are important.

The following describes the contribution of a positive difference density peak to the DDQ-P score for atom i,

$$\text{DDQ-P} = (\rho_p - 2)^2 \frac{(\text{RMAX}_p - R_i)}{\text{RMAX}_p}\left(0.5\frac{B_i}{B_{max}} + 0.5\right), \quad (3)$$

where ρ_p is the relative HDM peak height in σ, (only peaks above 3.0σ being used), RMAX_p is the cutoff distance in Å from positive difference peak to atom i and is dependent on the chemical nature of atom i (see Table 1) and R_i, B_i and B_{max} are as described for DDQ-W_{polar}.

The DDQ-P score is only calculated for positive difference density peaks located within a cutoff radius RMAX_p from the atom i under consideration.

Similarly, for negative peaks that are within the cutoff distance (RMAX_n) of atom i, the contribution to the DDQ-N value of atom i is

$$\text{DDQ-N} = (\rho_n + 2)^2 \frac{(\text{RMAX}_n - R_i)}{\text{RMAX}_n}\left(0.5\frac{B_i}{B_{max}} + 0.5\right), \quad (4)$$

where ρ_n is the relative HDM peak height in σ, (only peaks below -3.0σ being considered), RMAX_n is the cutoff distance in Å from negative difference peak to atom i and is dependent on the chemical nature of the atom i (see Table 1),and R_i, B_i and B_{max} are as described for DDQ-W_{polar}.

The dependence of the DDQ-P and DDQ-N scores on the (positive or negative) relative peak height has been made quadratic for peaks above or below a certain minimum value. The distance dependence is linear; the further away a distance density peak is, the less impact it has on the structure-quality indicator.

The rather large cutoff distances listed in Table 1 do result in double counting of peaks when calculating DDQ-P or DDQ-N scores for neighboring atoms. However, the rather large cutoff distances are needed to capture model errors other than those resulting in shift peaks. This is the case, for example, when an atom is either positioned too close to a real water peak or bonded to an atom which was not included in the model. The DDQ-P and DDQ-N scores are by no means an attempt to quantify mathematically the precise coordinate error of an atom owing to the presence of nearby shift peaks; these two scores are merely an indicator of the 'flatness' of the difference density around atoms.

2.2. Quality indicators per residue

The DDQ-P, DDQ-N, DDQ-W_{polar} and DDQ-W_{apolar} scores calculated for each atom are subsequently summed for each main-chain, side-chain and hetero or ligand moiety, and normalized with regard to the number of atoms of the moiety. The DDQ-W score for a particular moiety is defined as the sum of the average DDQ-W_{polar} and DDQ-W_{apolar} scores for that moiety. Similarly, the average 'shift-peak' scores DDQ-P and DDQ-N are summed, resulting in one combined DDQ-S score (*DDQ* shift-peak score). Therefore, it is sufficient to consider just the DDQ-W and DDQ-S scores when judging the correctness of a side-chain, main-chain or hetero or ligand moiety using *DDQ*. DDQ-W values should be high, DDQ-S values should be low. In fact, every residue with a positive DDQ-S value deserves individual inspection.

2.3. Global structure-quality indicators

The DDQ-W, DDQ-S, DDQ-P and DDQ-N scores obtained for each atom are used to arrive at average global *DDQ* structure-quality indicators. The respective *DDQ* scores for all atoms in the model are simply summed and divided by the total number of 'main-chain equivalents' (*i.e.* the total number of atoms in the model divided by four), resulting in overall DDQ-W, DDQ-S, DDQ-P and DDQ-N scores for a particular structure. This normalization puts the overall quality indicators on the same scale as the indicators for individual residue main-chain groups (which are comprised of four atoms), thus making it easier to compare the global scores and the local main-chain scores.

One of the more useful of these four different average DDQ scores is the average DDQ-W score, as will be seen below. This probably arises from the fact that the average DDQ-W score is dependent on both local and global structural accuracy, since it measures how well the overall model arrives at phases which can generate correct water peaks in the hydrated difference map that are subsequently stereochemically evaluated at a local level with respect to the model.

2.3.1. Difference density quality ratio. Another useful global quality indicator for crystal structures is DDQ-R (difference density quality ratio). The DDQ-R score is obtained by dividing the average DDQ-W by DDQ-S and

Table 2
Summary of the visual inspection of the electron density for the six side-chain and four main-chain moieties of the 1MPT structure that received the worst (highest) DDQ-S scores.

(*a*) Side chains

Side chain	DDQ-S	Main contributing HDM peak(s)	Problem	Solution
Gln137	8.8	-5.0σ peak	Incorrect side-chain position, incorrect temperature factors (average B = 18.5 Å^2), or incorrect protein sequence	Check protein sequence and mass or re-refine B factors, since there is no clear positive density above 2σ for this side chain in omit map
Glu112	5.2	-4.3σ peak	Slightly incorrect conformation	Readjust conformation in omit map
Pro56	4.5	-3.9σ peak	Residue out of register	Refit residues 56–58 (see Fig. 2*c*)
Arg275	4.3	-4.5σ peak	Incorrect conformation	Refit side chain in unambiguous omit map (see Fig. 2*a*)
Asn173	3.8	-4.3σ peak	Incorrect side-chain position	Refit side chain
His64	3.6	-4.1σ peak, $+3.9\sigma$ peak	Slightly incorrect conformation and also second conformation in omit map	Improve side-chain conformation; model second histidine conformation

(*b*) Main-chain moieties

Main chain	DDQ-S	Main contributing HDM peak(s)	Problem	Solution
Thr58	8.7	-4.9σ peak	Thr58 loops out of omit density	Refit residues 56–58 (see Fig. 2*c*)
Leu257	4.2	-4.1σ peak	Carbonyl oxygen is placed outside omit density	Refit residue; however, omit density does not give a clear indication of a carbonyl bump
Glu271	3.5	-4.1σ peak	Incorrect peptide orientation	Flip peptide (Fig. 2*b*)
Gly193	3.2	-3.1σ peak	B factor of 5.0 Å^2 too low, as omit density parameter is discontinuous at 3.0σ	Adjust B-factor refinement

appears to be even more sensitive, as we will see below, as an indicator of the global correctness of a crystal structure than the average DDQ-W score alone. This extra sensitivity is most likely to arise from the fact that the correct structure will have a high DDQ-W score combined with a low DDQ-S score, yielding a high DDQ-R for a correct structure and a low DDQ-R for a structure with significant errors.

2.3.2. Remaining positive density features. An additional global indicator, called the UFO (Unassigned Features left Over) score, can be derived from positive peaks which neither are close to the correct protein atoms nor are water peaks. The UFO score is based on the number of such extra positive density peaks in the hydrated difference map. Such as yet unassigned positive peaks could be due to parts of the protein structure that have not been modelled, ranging from a large side chain built as a small one or the omission of a ligand to the neglect of an entire domain.

In order to calculate the UFO score, great care needs to be taken to prune the list of positive peaks in the hydrated difference map. To this end, all peaks within RMAX_p from protein atoms and water peaks are removed. The removed water peaks include not only those properly positioned with respect to protein atoms, *i.e.* the first hydration shell, but also other potential water peaks in the next hydration shells. The criteria for a positive HDM peak to belong to a next hydration shell include a peak height above 3σ, a distance between 2.4–3.4 Å from a previously identified water peak and the absence of negative or positive peaks within 2.4 Å. From the eventual list of crystallographically unique unassigned positive peaks, the overall UFO score is calculated as

$$\mathrm{UFO} = [\textstyle\sum(\rho - 2)^2]/(n_{\mathrm{tot}}/4), \qquad (5)$$

where ρ is the relative peak height in the hydrated difference map and n_{tot} the total number of non-H atoms present in the structure.

3. Results and discussion

DDQ has been tested for its power to detect errors at the local as well as global level on a wide variety of proteins and in different resolution ranges. Some of the results obtained are described below.

3.1. *DDQ* as a local quality indicator of protein structures

As a first step in assessing the value of *DDQ*, several randomly chosen well refined structures from the Protein Data Bank were analysed. It appeared that the structure with PDB identifier 1MPT is a good case to illustrate the ability of *DDQ* to detect local errors. The 1MPT structure has been determined at 2.4 Å resolution and the R factor was 18.9%. In agreement with this low R factor are the reasonable overall *DDQ* statistics for this structure: DDQ-W = 3.6 and DDQ-R = 12.4 (for a comparison of these values see §3.2). However, at a local level, this structure appeared to need some improvement, since the positive DDQ-S scores calculated for a substantial number of main chains and side chains suggest that these particular moieties may have been modelled incorrectly (Table 2). These main chains and side chains were each checked in electron-density maps to see whether their high DDQ-S score was indeed the result of an error in the model.

In all instances, this appeared to be the case (Table 2). The verification consisted of a visual inspection of the positive and negative HDM density, as well as of an omit HDM map in which the residue itself and its two neighboring residues were omitted from the structure-factor calculation. Several examples of such informative electron-density inspections are shown in Fig. 2. Some of the shortcomings reported by high *DDQ* scores are as follows.

(i) The C-terminal residue Arg275 of the 1MPT structure has a side-chain DDQ-S score with a value of 4.3 (Table 2*a*) which is a high value. The difference Fourier map and an omit map reveal that the Arg275 side-chain conformation in this structure has incorrect dihedral angles. The omit electron-density maps clearly show the density for the correct conformation of Arg275 (Fig. 2*a*).

(ii) The main-chain moiety of Glu271 received quite a high main-chain DDQ-S score of 3.5 (Table 2*b*). This residue is located in a small helix but its main chain does not adopt the proper conformation: the peptide moiety is flipped and the carbonyl O atom is consequently pointing in the wrong direction (Fig. 2*b*). The correct position of the carbonyl O atom of Glu271 is evident from the omit electron density which distinctly shows a carbonyl bump (Fig. 2*b*). The correct conformation of Glu271 was modelled to demonstrate that the rebuilt Glu271 main chain does indeed fit much better into the omit electron density than the original model (Fig. 2*b*).

(iii) A particularly interesting region of model shortcomings identified by *DDQ* involved residues near residue Thr58. The main chain of this residue received the structure's highest main-chain DDQ-S score of 8.7 (Table 2*b*). Visual inspection of the electron-density maps reveals that the main chain of Thr58 is embedded in negative HDM density and loops out of the omit electron density (Fig. 2*c*). Pro56 also received a significant positive side-chain DDQ-S score of 4.5 (Table 2*a*). The position of both residues Pro56 and Ser57 were in error and the model appeared to be out of register by one residue. The correct position of residues 56–58 could easily be obtained by manual rebuilding, and once rebuilt these residues fit the omit electron density much better than the deposited structure (Fig. 2*c*).

The program *DDQ* has thus been shown to correctly and rapidly identify several significant local errors, including a frame-shift error, in a deposited 2.4 Å crystal structure with a low *R* factor unfamiliar to the authors of the current paper. Three of the errors described in Table 2 (His64, Glu112 and Gly193) did not appear to be obvious using other structure-verification programs such as the real-space correlation coefficient (Jones *et al.*, 1991) or *PROCHECK* (Lawskowski *et al.*, 1993).

The *DDQ* program was designed to not only pinpoint errors in crystal structures but also identify residues whose positions can be treated with great confidence owing to the presence of well positioned neighbouring HDM water peaks. An example of this is depicted in Fig. 3, showing residues 42–44 of the 1MPT structure mentioned above. The main-chain moieties of residues Leu42, Asn43 and Ile44 received very favourable DDQ-W scores of 21.4, 18.0 and 8.2 respectively (their DDQ-S scores were all 0.0). These scores are indicative of a well fitted

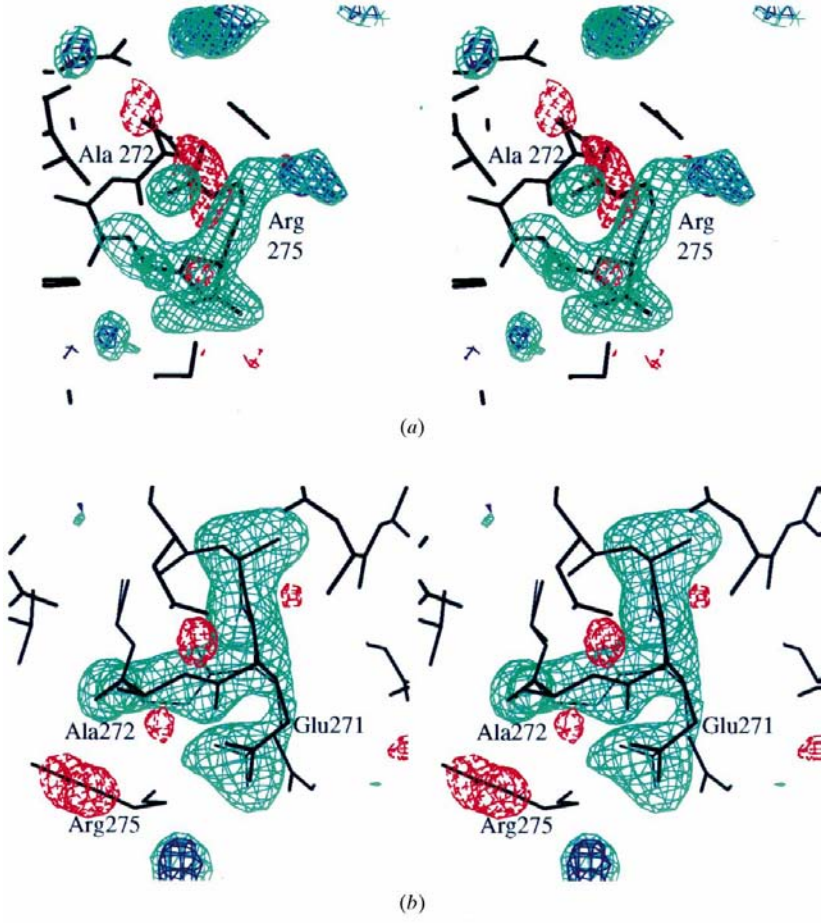

Figure 2
Electron-density maps showing several incorrectly modelled regions in the 1MPT structure. (*a*) Superposition of different types of electron-density maps calculated around Arg275 of 1MPT. All the electron-density maps shown in this manuscript did not include waters in the structure-factor calculation, including the omit electron-density maps. The positive hydrated $|F_{obs}| - |F_{calc}|$ density at 3σ is shown as solid blue lines and the negative $|F_{obs}| - |F_{calc}|$ density at -3σ is shown as broken red lines. A hydrated $|F_{obs}| - |F_{calc}|$ omit map in which the two terminal residues 274–275 have been omitted from the structure-factor calculation is shown as green lines contoured at 2.5σ. Note that this omit map reveals that the guanidinium group has been originally positioned incorrectly in a water peak. This peak is within good hydrogen-bonding distance from the carbonyl O atom of residue Ala272 and is actually a water molecule. (*b*) Superposition of different types of electron-density maps calculated around Glu271 of 1MPT. The positive hydrated $|F_{obs}| - |F_{calc}|$ density at 3σ is shown as solid blue lines and the negative $|F_{obs}| - |F_{calc}|$ density at -3σ is shown as broken red lines. A hydrated $|F_{obs}| - |F_{calc}|$ omit map, in which the two terminal residues 270–272 have been omitted from the structure-factor calculation, is shown as green lines contoured at 2.5σ. The original 1MPT coordinates are shown as thin lines, while the manually rebuilt model is shown as thick lines. Glu271 is situated near the incorrectly modelled residue Arg275 highlighted in Fig. 2(*a*).

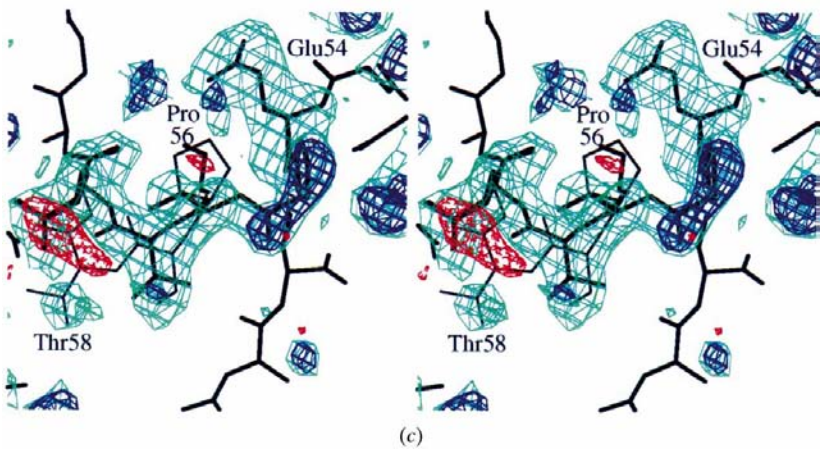

Figure 2 (continued)

(*c*) Difference and omit electron-density maps calculated around residues 56–58 of 1MPT. The positive hydrated $|F_{obs}| - |F_{calc}|$ density at 3σ is shown as blue solid lines and the negative $|F_{obs}| - |F_{calc}|$ density at -3σ as broken red lines. A $|F_{obs}| - |F_{calc}|$ omit map, in which residues 54–59 have been omitted from the structure-factor calculation, is depicted in solid green lines contoured at 2.0σ. The original 1MPT coordinates are shown as thin lines, while the manually rebuilt model is shown as thick lines. The PDB header of the 1MPT structure reports that residue 55 is deleted from the protein sequence and, therefore, there is a gap in the sequence numbering resulting in an unconnected Glu54 and Pro56. The positions of the incorrectly modelled residues Pro56 and Thr58 are labelled as well as residue Glu54.

region of the model, as is evident from the omit map as well as the hydrated difference maps which shows that the backbone O atoms and N atoms of residues 42–44 are surrounded by many water molecules at the proper positions (Fig. 3).

Next, it was tested whether the *DDQ* program could detect errors in a high-resolution crystal structure. Obviously, high-resolution structures are significantly less prone to errors since the electron-density maps are very detailed allowing, in most cases, an unambiguous positioning of residues. However, *DDQ* was able to detect a (small) error in a randomly chosen high-resolution crystal structure from the PDB: the 2AYH structure determined at 1.6 Å. The R and R_{free} values for this well refined structure are 14.3 and 22.0%, respectively. The excellent quality of this structure is also reflected in the high DDQ-W and DDQ-R scores which are 25.3 and 74.6, respectively. However, the side chain of Ser90 has been modelled as only partially correct. This serine side chain received a DDQ-S of 4.8 owing to the presence of a 4.3σ HDM peak at 1.4 Å distance from its O^{γ} atom (Fig. 4). This positive peak suggests that Ser90 adopts two different conformations, of which only one is included in the model. The presence of the second alternative conformation for the Ser90 side chain is confirmed by the omit electron density, which clearly shows an additional bump for the O^{γ} atom (Fig. 4). Residue Ser90 thus adopts two different conformations which could both be included in the final model and thereby describe the crystal structure even more accurately than the deposited coordinates. Interestingly, the O^{γ} atom of Ser90 in the alternative conformation is at a good hydrogen-bonding distance to a nearby water molecule (Fig. 4). Similar to somez of the errors in the 1MPT structure, this error was not obvious from other structure-quality indicators. *DDQ* has thus been shown to identify a (minor) error in a high-resolution structure and thus appears also to be useful for further improvement of virtually correct high-resolution crystal structures.

Combined with several other cases (not described here), including detecting errors in a 2.8 Å resolution structure, it appears that *DDQ* is able to accurately detect local errors in deposited crystal structures over a broad resolution range. Also, a wide variety of local model errors can be detected by *DDQ* regarding atomic positions and thermal parameters as well as missing or incomplete parts of the model.

3.2. *DDQ* as a global-quality indicator of protein structures

To be useful, a global structure-validation indicator should obviously be sensitive to the average coordinate error of a structure. The effect of the coordinate error on all average *DDQ* scores has been tested with the 2.3 Å structure of heat-labile enterotoxin I (LT-I) complexed with lactose (Sixma *et al.*, 1992; PDB identifier 1LTT) as the model system. To generate a set of structures with varying coordinate errors, the program *X-PLOR* (Brünger *et al.*, 1987) was used to perturb the original structure by performing slow-cooling molecular-dynamics runs without using X-ray restraints. A range of coordinate errors was introduced by using different starting temperatures for these runs. Subsequently, all the different structures were evaluated using the *DDQ* program. The resulting average DDQ-P and DDQ-N scores are plotted *versus* coordinate error in Fig. 5(*a*), as are the DDQ-W and DDQ-R scores (Fig. 5*b*).

Both the average DDQ-P and DDQ-N scores initially increase with increasing coordinate error but then level off. Once the model deviates more than 0.8 Å on average from the starting crystal structure, these two scores then slowly decrease with increasing coordinate error (Fig. 5*a*). The initial upward trend of DDQ-P and DDQ-N as the coordinate error increases arises from the increasing appearance of shift peaks close to atoms, the position of which deviate significantly from the initial correct position. This trend continues until the model deviates too far from the crystal structure and the resulting phase error is too large to correctly 'highlight' all the mispositioned atoms by means of shift peaks in a difference Fourier map.

The second set of *DDQ* scores, DDQ-W and DDQ-R, behave as expected with increasing coordinate error. Both scores decrease as the model increasingly deviates from the correct structure (Fig. 5*b*). The decreasing trend of DDQ-W is a consequence of the synergistic effect of the increase in phase error, causing the water peak heights to be lower, coupled with the deterioration of the stereochemical alignment of the model with respect to these water peaks. The even sharper

decreasing trend of the DDQ-R score with increasing coordinate error arises from the additional effect of the increasing appearance of shift peaks near incorrectly positioned atoms as discussed above. The observed sensitivity of the DDQ-R score with respect to coordinate error is very good; an increase in the overall coordinate error of 0.25 Å decreases the DDQ-R score by about 85% (Fig. 5*b*), while the *R* factor only increases by 5% (Fig. 5*c*).

Another measure of the global accuracy of a crystal structure is its phase error. Therefore, the overall average phase error of each of the obtained models was calculated (using *X-PLOR*) and the DDQ-W and DDQ-R scores were plotted against this phase error (Fig. 5*d*). An increase in phase error of 15° caused a very significant drop in the two DDQ scores. In conclusion, unlike the DDQ-P and DDQ-N scores, the DDQ-W and DDQ-R scores are sensitive and useful indicators of the overall coordinate error and phase error of a 2.3 Å resolution crystal structure.

The general usefulness of DDQ-W and DDQ-R as indicators of the overall coordinate error was also tested on other structures determined at resolutions differing from the 2.3 Å in the previous case of 1LTT. For this test two structures were chosen randomly from the PDB. The first structure (PDB identifier 2AYH) has been refined at high resolution (1.6 Å) while the second structure (PDB identifier 1PBC) has been refined at moderate resolution (2.8 Å). To generate structures with increasing coordinate error, both structures were subjected to the same protocol as described previously for 1LTT. These perturbed structures were used to determine their DDQ-W and DDQ-R scores, which were then plotted against coordinate error. The observed decreasing trend of both these DDQ scores (not shown) is found to be conserved and similar to Fig. 5(*b*). These results suggests that the DDQ-W and DDQ-R scores are useful for analysing crystal structures over a broad resolution range extending from high resolution to 2.8 Å resolution.

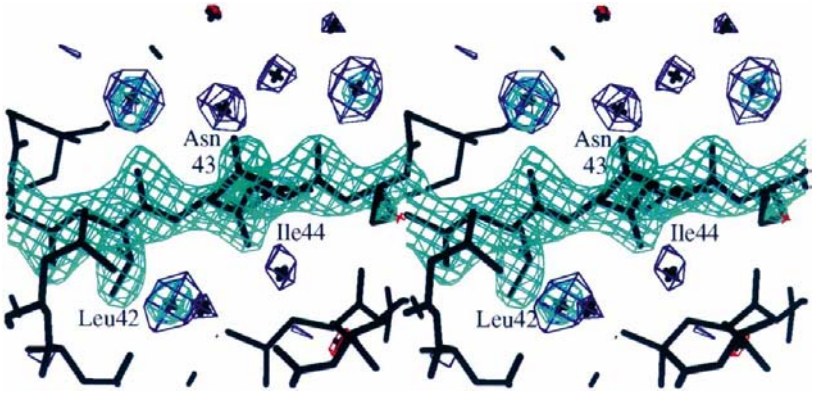

Figure 3
Electron-density maps showing a correctly modelled stretch of residues in the 1MPT structure. Difference and omit electron-density maps are calculated around residues 42–44 of 1MPT. The positive hydrated $|F_{obs}| - |F_{calc}|$ density at 3σ is shown as solid blue lines and the negative $|F_{obs}| - |F_{calc}|$ density at -3σ is shown as red lines. A hydrated $|F_{obs}| - |F_{calc}|$ omit map, in which the residues 41–45 have been omitted from the structure-factor calculation, is shown as green lines contoured at 3.5σ. HDM peaks above 3σ and below -3σ are indicated by a black cross.

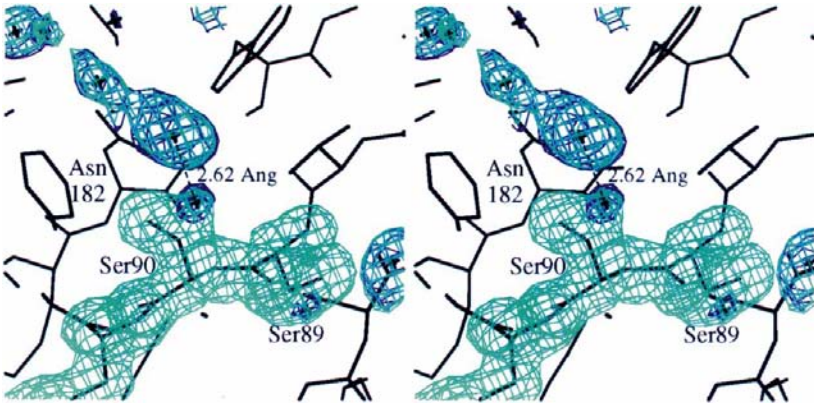

Figure 4
Difference and omit electron-density maps calculated around Ser90 of the 2AYH structure. The positive hydrated $|F_{obs}| - |F_{calc}|$ density at 3σ is shown as solid blue lines and the negative $|F_{obs}| - |F_{calc}|$ density at -3σ is shown as broken red lines. A hydrated $|F_{obs}| - |F_{calc}|$ omit map in which residues 89–91 have been omitted from the structure-factor calculation is shown in green lines contoured at 3σ. The O^{γ} atom of Ser90 is making a 2.6 Å hydrogen bond with the O^{δ} atom of Asn182 (hydrogen bond not drawn). The positive 4.3σ peak near Ser90 represents an alternative second position for the O^{γ} atom of this side chain. This peak is situated at 2.6 Å from a strong water density peak and at 3.0 Å distance from the O^{δ} atom of Asn182.

The calculated DDQ-W and DDQ-R scores for all 106 structures are plotted logarithmically in Figs. 6(*a*) and 6(*b*), respectively. The scatter plot of DDQ-W score *versus* resolution establishes the previously noted resolution dependence of the DDQ-W score. At high resolution significantly higher values are seen than at lower resolution. This resolution dependence is inherent to higher resolution structures which are, in general, not only more accurately determined but are also able to produce electron-density maps that display small electron-density features, such as water molecules, significantly more strongly.

Similar to the DDQ-W scatter plot, the DDQ-R scatter plot also follows a declining trend with decreasing resolution (Fig. 6*b*). This is somewhat surprising, since both the numerator and denominator of DDQ-R are dependent on elec-

tron-density features which should both be resolution dependent. The observed resolution dependence of DDQ-R is most likely to be a consequence of the fact that the water peaks (in the numerator) are, in most cases, the strongest features in the HDM. The numerator of DDQ-R apparently dominates, resulting in a somewhat similar resolution trend for DDQ-R as seen for DDQ-W.

The ranking of the global *DDQ* scores for new structures to be validated is carried out using the 106 data points present in Fig. 6. The data points are grouped in resolution shells of 0.2 Å comprising ten data points per bin (except for the highest and lowest resolution bin, owing to the limited availability of coordinates accompanied by structure factors from the PDB at those resolutions). For each bin, the average DDQ-W (and DDQ-R) is calculated as well as the average of the top half (yielding the top 25 percentile boundary) and average of the bottom half (yielding the bottom 25 percentile boundary) (see Table 3). *DDQ* uses these values, as well as the lowest and highest score in each bin (see Fig. 6), to rank new structures to be validated. The ranking order of each overall *DDQ* score is therefore output as follows: better than any of the ten test structures, within the top 25%, above average, below average, within the bottom 25%, or worse than any of the ten test structures in that particular resolution bin.

Obviously, the dependence of the global DDQ-W and DDQ-R scores on the presence of water peaks in the HDM makes these scores unfortunately of less use beyond a certain resolution where water molecules can no longer be observed. The data in Table 3 suggests that this resolution limit is approximately 2.9 Å, as the average DDQ-W and DDQ-R

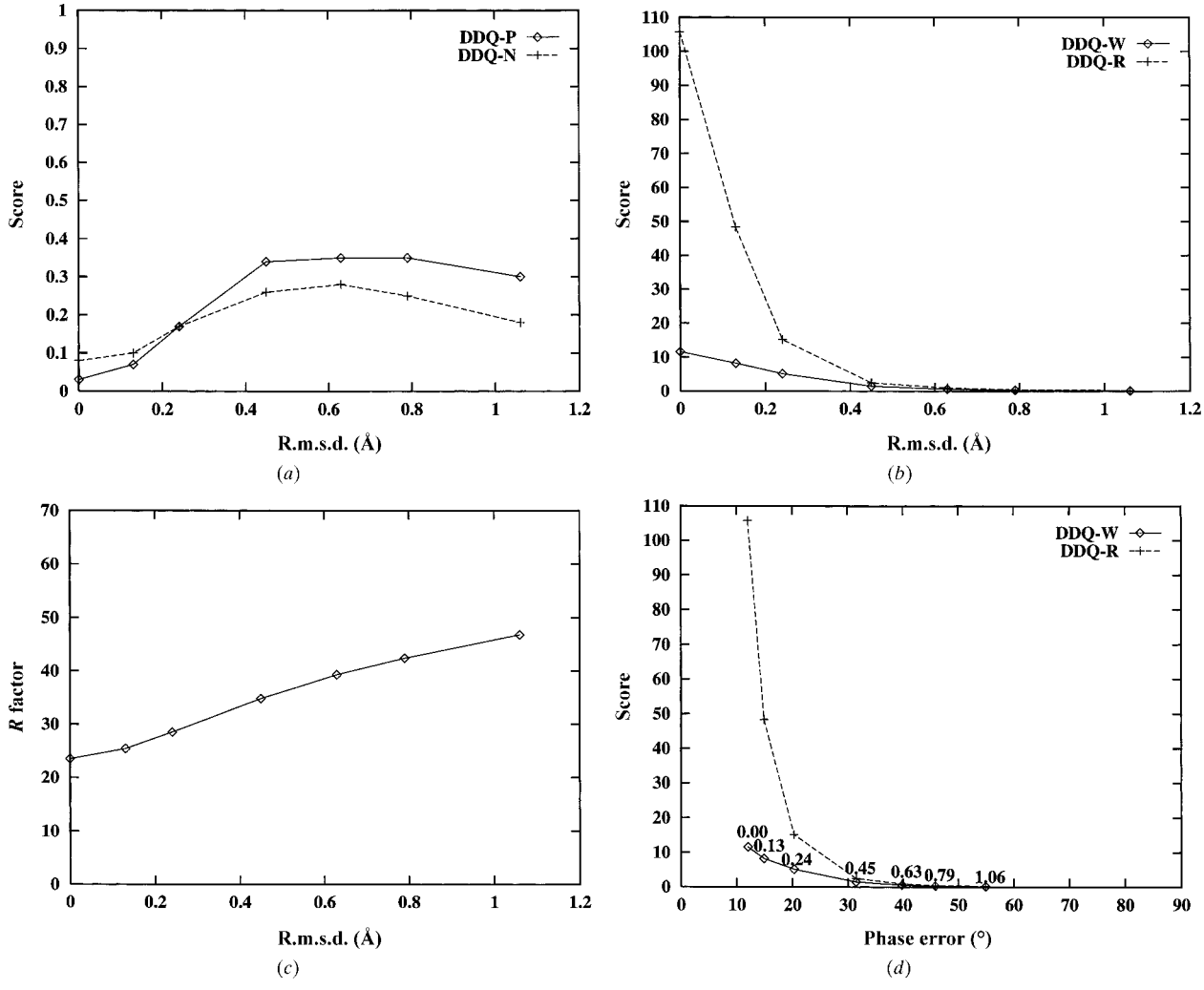

Figure 5
DDQ scores as function of coordinate error and phase error. (*a*) DDQ-P and DDQ-N as function of random coordinate error for 1LTT. The DDQ-P score is plotted as a solid line and the DDQ-N score is represented by a dashed line. The r.m.s. deviations for the structures that were obtained are 0.00, 0.13, 0.24, 0.45, 0.63, 0.79 and 1.06 Å. The same coordinate sets are used in (*a*)–(*d*). (*b*) DDQ-W and DDQ-R scores as function of randomly introduced coordinate error for 1LTT. The DDQ-W score is plotted as a solid line and the DDQ-R score is represented by a dashed line. (*c*) The *R* factor as a function of randomly introduced coordinate error for 1LTT. The *R* factor starts at 23.5%, even though the *R* factor reported for this structure is 17.7%. This discrepancy is due to the fact that the generated structures, including the starting structure, did not contain any water molecules. (*d*) DDQ-W and DDQ-R scores as function of the average phase error for 1LTT. The DDQ-W score is plotted as a solid line and the DDQ-R score is represented by a dashed line. The phase error is the phase difference between the generated models and the correct model including its water molecules. Since these generated models did not include waters, the calculated phase error starts around 12° for the unperturbed structure.

Table 3
Average values of the global DDQ scores as function of resolution.

Average values for DDQ-W, DDQ-R and UFO score are given for each resolution bin as well as average values for the top half (yielding the top 25 percentile value) and bottom half (yielding the bottom 25 percentile value) of each of the scores are listed. Each bin contains ten data points except for the last resolution bin which consists of six data points.

Resolution bin		DDQ-W score			DDQ-R score			UFO score		
Start	End	Average	Top 25%	Bottom 25%	Average	Top 25%	Bottom 25%	Average	Top 25%	Bottom 25%
0.89	1.49	41.8	56.5	27.2	39.0	61.6	16.4	1.47	2.59	0.35
1.50	1.69	28.5	43.5	13.5	47.1	81.3	12.0	0.67	0.89	0.46
1.70	1.89	19.7	28.3	11.1	37.7	58.1	17.4	0.44	0.63	0.24
1.90	2.09	7.5	10.8	4.3	19.9	31.9	8.0	0.29	0.48	0.11
2.10	2.29	4.7	7.3	2.1	13.5	23.2	3.9	0.37	0.59	0.15
2.30	2.49	4.2	6.7	1.7	15.3	27.9	2.7	0.20	0.27	0.12
2.50	2.69	2.5	4.0	0.9	8.5	13.2	3.7	0.21	0.34	0.08
2.70	2.89	1.3	2.0	0.5	6.6	11.9	1.4	0.13	0.17	0.09
2.90	3.09	0.4	0.6	0.1	0.8	1.3	0.2	0.07	0.10	0.04
3.10	3.29	0.2	0.4	0.03	0.5	0.8	0.07	0.11	0.16	0.06
3.30	3.50	0.06	0.09	0.02	0.1	0.2	0.05	0.13	0.21	0.05

scores both drop dramatically in the resolution bin 2.9–3.09 Å compared with the scores in the 2.7–2.89 Å bin. This limit is also in agreement with the fact that the DDQ-W score of 1.5 for the 2.8 Å structure 1PBC mentioned above, was still sensitive to the introduction of model error (not shown) similar to the 1LTT example. In practical terms, a resolution limit of better than 2.9 Å would exclude less than 10% of the structures currently in the PDB from validation using the program *DDQ*.

Although the DDQ-W score appears applicable to the validation of protein structures, we observed surprisingly low scores for quite a number of uncomplexed DNA and RNA structures (data not shown). Upon inspection of the relevant coordinate files in order to uncover the reason for this discrepancy between proteins and nucleic acids, we noticed that in most cases the temperature factor for the waters in nucleic acid structures were on average about 30 Å^2 higher than for the rest of the atoms. This temperature-factor spread is considerably less for protein-crystal structures, suggesting that DNA or RNA does not bind water as tightly as proteins, possibly as a result of a significantly decreased tendency to form hydrophilic water cavities. As a result, the water molecules in DNA and RNA structures might be more mobile on average, resulting in lower HDM peak heights for these waters, which causes the DDQ-W score to be significantly lower for nucleic acids than for proteins. However, several protein–DNA complexes were included in the test set of 106 structures and did receive global *DDQ* scores which were comparable to proteins: 7ICG at 3.0 Å (DDQ-W score of 1.1, which is the best score in its resolution bin) and 1AIS at 2.1 Å (DDQ-W score of 2.1, which is close to the bottom 25% boundary for its resolution bin).

Interestingly, global *DDQ* scores comparable to average were also obtained for two integral membrane protein structures found in the test set of 106 structures. The structures of the light-harvesting complex (1KZU at 2.5 Å) and OMPF porin (2OMF at 2.4 Å) received global DDQ-W scores of 3.9 (above average) and 12.3 (best of the ten in its resolution bin), respectively. This is despite the fact that membrane proteins tend to have less surface exposed to water and are therefore expected to contain fewer potential water-binding sites than water-soluble proteins.

In summary, the DDQ-W and DDQ-R scores have both been shown to be useful as indicators for the global accuracy of protein crystal structures. A cautious resolution limit for their use is better than 2.9 Å, although well refined structures determined up to 3.2 Å have been observed to still receive significant global *DDQ* scores. The program *DDQ* can be used for validating protein–DNA complexes and integral membrane proteins but the use of *DDQ* for validating uncomplexed DNA (or RNA) structures is not quite satisfactory, which is probably a consequence of the rather high *B* values of water molecules in the crystal structures of oligonucleotides.

3.3. *DDQ* as a tool to monitor model incompleteness

A quantitative measure of completeness of a model is useful for potential users of the coordinates, as well as for the crystallographer who might like to check whether there are still missing parts of the structure. An incomplete structure will yield significant extra positive difference density arising from the unintentionally omitted atoms. The presence of these additional positive peaks forms the basis of the UFO score for the diagnosis of the degree of incompleteness of structures. To test the ability of the UFO score to sense whether a structure is missing a medium-sized ligand, the 1.8 Å crystal structure of the 15 kDa cellular retinoic acid binding protein type II complexed with all-*trans* retinoic acid (PDB identifier 1CBS) was used as a test case (structure factors were kindly provided by Dr Gerard Kleywegt). Two hydrated difference maps were calculated. One used the complete model whilst the second omitted the all-*trans* retinoic acid ligand from the structure-factor calculation. Subsequently, both the complete and incomplete structures were evaluated by the *DDQ* program using their corresponding hydrated differences maps. The resulting UFO scores are surprisingly sensitive to the partial incompleteness of a model. Leaving out the ligand, which

corresponds to omitting only 2% of the atoms in the structure, increased the UFO score by more than 230% from 0.44 to 1.46. For comparison, the average UFO score calculated for the ten structures in the corresponding resolution bin is 0.44 (see Table 3) and the highest UFO score in this bin was 0.86. Most interestingly, the global-quality indicators DDQ-W and DDQ-R are also significantly affected by omitting the ligand: the DDQ-W score decreased from 22.8 to 15.6 while the DDQ-R score dropped from 45.7 to 34.4. The reason why these two global *DDQ* scores change so dramatically by omitting just a 22-atom ligand from a 1091-atom protein is probably the decrease in quality of the map; omitting the ligand from the structure-factor calculations will increase the phase error, causing the map to become noisier, and thus decreasing the critical peak heights of the water peaks. In summary, the UFO score is a sensitive indicator of an incomplete model and is a valuable addition to the DDQ-W and DDQ-R scores for the assessment of the global accuracy of a crystal structure.

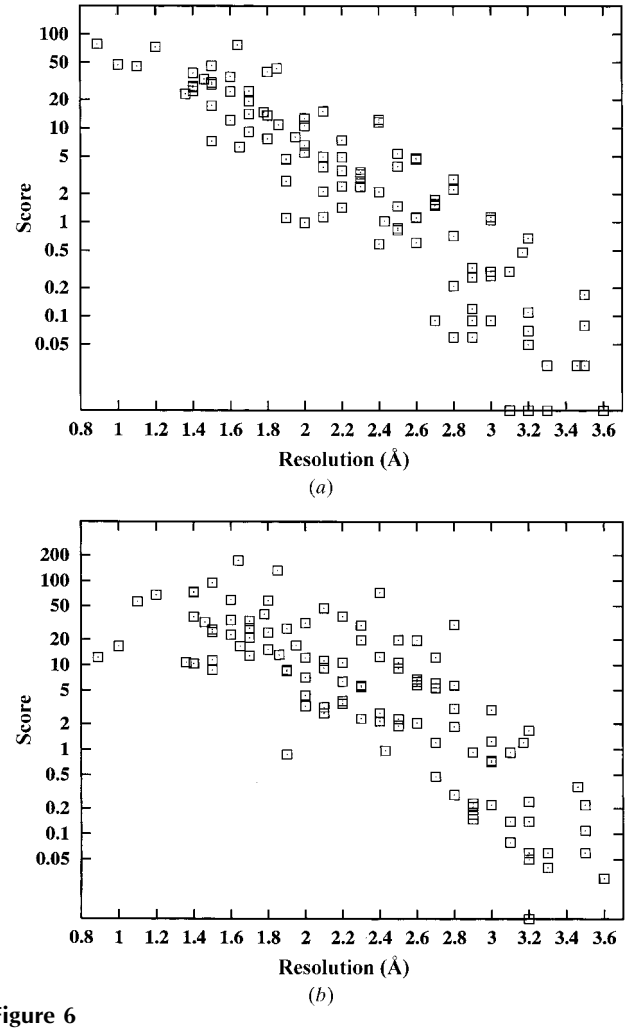

Figure 6
DDQ scores as function of resolution. (*a*) Scatter plot of DDQ-W against resolution of randomly selected PDB structures. The data is plotted logarithmically and contains the DDQ-W score of 106 structures from the PDB listed in decreasing resolution: 1AB1, 8RXN, 1IGD, 1RGF, 1RHS, 194L, 1G3P, 1ST3, 1SVN, 2CTC, 1AIE, 1AKI, 1RIE, 2ARC, 2CTB, 1BKF, 1MYR, 1PHP, 1RA2, 2AAC, 1FEC, 1TOP, 1VHH, 1YAL, 2ABH, 1AOQ, 1CGH, 1LML, 1QBA, 2NAC, 1AQ6, 1AT0, 1FIP, 1JUG, 1XPB, 1LCI, 1MJC, 2CHB, 2EMD, 2PGD, 1ACC, 1AIS, 1KIP, 1OIL, 1SFE, 1DBP, 1GNW, 1PCZ, 1TUL, 1VSI, 1AR0, 1HBV, 1OXM, 2BNH, 4MON, 1ECE, 1MRC, 2ADA, 2OMF, 4FUA, 1BMG, 1KZU, 1PAW, 1YTJ, 2ACE, 1AF4, 1AO5, 1CD8, 1JUY, 1RD7, 1CSQ, 1IOA, 1OFG, 1PBF, 3PBG, 1AVE, 1ESP, 1GIN, 1JSW, 4TMY, 1AGX, 1BLE, 1CTP, 1NCD, 1NLD, 1ADT, 1AGN, 1AY9, 1FSS, 7ICG, 1BMO, 1KXA, 1PGQ, 1VCQ, 1ADV, 1ATT, 1MPN, 1PCI, 1PYI, 1UWB, 1KOA, 1TGK, 1KCT, 1FCC, 1JCK, 1PGE. (*b*) Scatter plot of DDQ-R against resolution of randomly selected PDB structures. The data is plotted logarithmically and contains the DDQ-R scores from the same 106 structures.

4. Materials and methods

4.1. Map calculations and generation of peak lists

Electron-density maps were calculated using the programs *X-PLOR* (Brünger *et al.*, 1987) or the *CCP*4 suite of programs (Collaborative Computational Project, Number 4, 1994). The water molecules are deliberately removed from the structure-factor calculation prior to calculating the map. A low-resolution cutoff of 25 Å was used and no cutoff on intensities was applied. Subsequently, the *CCP*4 program *PEAKMAX* was used to read in the $|F_{obs}| - |F_{calc}|$ electron-density map covering the complete molecule and to write out the coordinates of all positive peaks above 3σ and negative peaks below -3σ (where σ is the r.m.s deviation from the mean density). The σ cutoff should reduce the number of noise peaks, since random error peaks in a difference map are less than 2.5–3.0σ (Ladd & Palmer, 1993). This peak list and the coordinate file of the crystal structure without the water molecules are the input for the *DDQ* program. The output of the program consists of several files containing the local and global *DDQ* scores. The latter scores are ranked, using the data points shown in Fig. 6, as better than any of the ten structures in the corresponding resolution bin, top 25%, above 50%, below 50%, bottom 25%, or worse than any of the ten test structures in the corresponding resolution bin (bins are in 0.2 Å shells). Note that limited completeness of the diffraction data set can also affect the overall *DDQ* scores. Tests on a highly complete 2.2 Å data set (99.8%) of 1TUL showed that the random omission of 5, 10, 20 or 30% of the reflections decreased the DDQ-W score by 7, 19, 24 and 29%, respectively, whereas the DDQ-R score decreased by 20, 38, 42 and 31%, respectively. The observed decrease of DDQ-W basically 'quantifies' the amount of information or signal in a difference map lost as data completeness decreases. This suggests that the score DDQ-W could also potentially be used as a difference-map quality indicator in a variety of other instances. For example, *DDQ* might be useful to see whether σ_A weights or a different scale factor between F_{obs} and F_{calc} (both useful in partial model cases) improve the quality of a difference map.

4.2. *DDQ* program

The *DDQ* program is written in Fortran-77 and is freely available by contacting Focco van den Akker (e-mail: focco@pierre.hh.ri.ccf.org).

We would like to thank Vivien Yee, Rachel Klevit, and Dave Teller for critical reading of the manuscript and Gerard Kleywegt for providing the structure factors for 1CBS. This research was supported by the NIH (AI34501) and by an equipment grant from the Murdock Charitable Trust to the Biomolecular Structure Center.

References

Baker, E. N. & Hubbard, R. E. (1984). *Prog. Biophys. Mol. Biol.* **44**, 97–179.
Brändén, C.-I. & Jones, T. A. (1990). *Nature (London)*, **343**, 687–689.
Brünger, A. T. (1992). *Nature (London)*, **355**, 472–475.
Brünger, A. T., Kuriyan, J. & Karplus, M. (1987). *Science*, **235**, 458–460.
Collaborative Computational Project, Number 4 (1994). *Acta Cryst.* D**50**, 760–763.
Colovos, C. & Yeates, T. O. (1993). *Protein Sci.* **2**, 1511–1519.
Cruickshank, D. W. J. (1996). *Refinement of Macromolecular Structures. Proceedings of the CCP4 Study Weekend*, edited by E. Dodson, M. Moore & S. Bailey, pp. 11–22. Warrington: Daresbury Laboratory.
Goodsell, D. S., Kopka, M. L. & Dickerson, R. E. (1995). *Biochemistry*, **34**, 4983–4993.
Gregoret, L. M., Rader, S. D., Fletterick, R. J. & Cohen, F. E. (1991). *Proteins*, **9**, 99–107.
Henderson, R. & Moffat, J. K. (1971). *Acta Cryst.* B**27**, 1414–1420.
Holm, L. & Sander, C. (1992). *J. Mol. Biol.* **225**, 93–105.
Hooft, R. W. W., Vriend, G., Sander, C. & Abola, E. E. (1996). *Nature (London)*, **381**, 272.
Jones, T. A., Kleywegt, G. J. & Brünger, A. T. (1996). *Nature (London)*, **383**, 18–19.
Jones, T. A., Zou, J.-Y., Cowan, S. W. & Kjeldgaard, M. (1991). *Acta Cryst.* A**47**, 110–119.
Kleywegt, G. J. & Brünger, A. T. (1996). *Structure*, **4**, 897–904.
Kleywegt, G. J. & Jones, T. A. (1996). *Structure*, **4**, 1395–1400.
Ladd, M. F. C. & Palmer, R. A. (1993). *Structure Determination by X-ray Crystallography*, 3rd ed., pp. 433–435. New York & London: Plenum Press.
Lawskowski, R. A., MacArthur, M. W., Moss, D. & Thornton, J. M. (1993). *J. Appl. Cryst.* **26**, 283–291.
Lüthy, R., Bowie, J. U. & Eisenberg, D. (1992). *Nature (London)*, **356**, 83–85.
Luzzati, P. V. (1952). *Acta Cryst.* **5**, 802–810.
McPhalen, C. A., Strynadka, N. C. J. & James, M. N. G. (1991). *Adv. Protein Chem.* **42**, 77–144.
Pitt, W. R. & Goodfellow, J. M. (1991). *Protein Eng.* **4**, 531–537.
Pontius, J., Richelle, J., Wodak, S. J. (1996). *J. Mol. Biol.* **264**, 121–136.
Ramakrishnan, C. & Ramachandran, G. N. (1965). *Biophys. J.* **5**, 909–933.
Read, R. J. (1986). *Acta Cryst.* A**42**, 140–149.
Read, R. J. (1990). *Acta Cryst.* A**46**, 900–912.
Roe, S. M. & Teeter, M. M. (1993). *J. Mol. Biol.* **229**, 419–427.
Sheldrick, G. M. (1995) *SHELXL*93*. A Program for the Refinement of Crystal Structures from Diffraction Data*. Intitute für Anorganische Chemie, Göttingen, Germany.
Sippl, M. J. (1993). *Proteins*, **17**, 355–362.
Sixma, T. K., Pronk, S. E., Kalk, K. H., van Zanten, B. A. M., Berghuis, A. M. & Hol, W. G. J. (1992). *Nature (London)*, **355**, 561–564.
Stout, G. H. & Jensen, L. H. (1989). *X-ray Structure Determination*, 2nd ed., pp. 349–354. New York: John Wiley & Sons.
Thanki, N., Thornton, J. M. & Goodfellow, J. M. (1988). *J. Mol. Biol.* **202**, 637–657.
Umrania, Y., Nikjoo, H. & Goodfellow, J .M. (1995). *Int. J. Radiat. Biol.* **67**, 145–152.
Walshaw, J. & Goodfellow, J. M. (1993). *J. Mol. Biol.* **231**, 392–414.